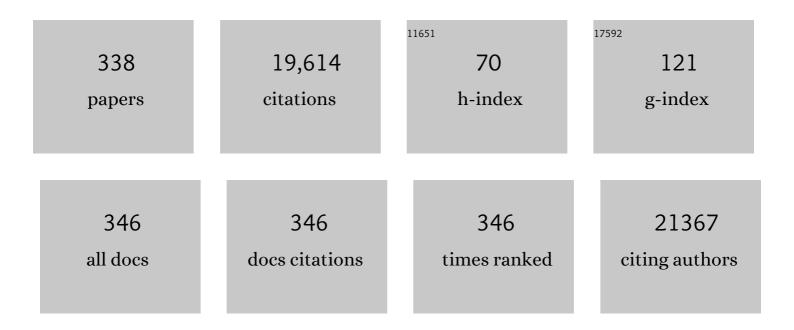
List of Publications by Year in descending order

Source: https://exaly.com/author-pdf/4863422/publications.pdf Version: 2024-02-01



FENC PENC

#	Article	IF	CITATIONS
1	Recent advances in metal sulfides: from controlled fabrication to electrocatalytic, photocatalytic and photoelectrochemical water splitting and beyond. Chemical Society Reviews, 2019, 48, 4178-4280.	38.1	810
2	Hybrids of Two-Dimensional Ti ₃ C ₂ and TiO ₂ Exposing {001} Facets toward Enhanced Photocatalytic Activity. ACS Applied Materials & Interfaces, 2016, 8, 6051-6060.	8.0	653
3	Phosphorusâ€Doped Graphite Layers with High Electrocatalytic Activity for the O ₂ Reduction in an Alkaline Medium. Angewandte Chemie - International Edition, 2011, 50, 3257-3261.	13.8	647
4	Mechanism study on adsorption of acidified multiwalled carbon nanotubes to Pb(II). Journal of Colloid and Interface Science, 2007, 316, 277-283.	9.4	346
5	Fractional purification and bioconversion of hemicelluloses. Biotechnology Advances, 2012, 30, 879-903.	11.7	338
6	Comparative Study of Hemicelluloses Obtained by Graded Ethanol Precipitation from Sugarcane Bagasse. Journal of Agricultural and Food Chemistry, 2009, 57, 6305-6317.	5.2	312
7	High efficiency photocatalytic hydrogen production over ternary Cu/TiO2@Ti3C2Tx enabled by low-work-function 2D titanium carbide. Nano Energy, 2018, 53, 97-107.	16.0	300
8	Synthesis and characterization of substitutional and interstitial nitrogen-doped titanium dioxides with visible light photocatalytic activity. Journal of Solid State Chemistry, 2008, 181, 130-136.	2.9	282
9	A hydrothermal etching route to synthesis of 2D MXene (Ti3C2, Nb2C): Enhanced exfoliation and improved adsorption performance. Ceramics International, 2018, 44, 18886-18893.	4.8	276
10	Preparation of cuprous oxides with different sizes and their behaviors of adsorption, visible-light driven photocatalysis and photocorrosion. Solid State Sciences, 2009, 11, 129-138.	3.2	266
11	Z-scheme Bi2WO6/CuBi2O4 heterojunction mediated by interfacial electric field for efficient visible-light photocatalytic degradation of tetracycline. Chemical Engineering Journal, 2019, 369, 292-301.	12.7	255
12	2H- and 1T- mixed phase few-layer MoS2 as a superior to Pt co-catalyst coated on TiO2 nanorod arrays for photocatalytic hydrogen evolution. Applied Catalysis B: Environmental, 2019, 241, 236-245.	20.2	242
13	Selective Catalysis of the Aerobic Oxidation of Cyclohexane in the Liquid Phase by Carbon Nanotubes. Angewandte Chemie - International Edition, 2011, 50, 3978-3982.	13.8	234
14	Nitrogen-, phosphorous- and boron-doped carbon nanotubes as catalysts for the aerobic oxidation of cyclohexane. Carbon, 2013, 57, 433-442.	10.3	209
15	Carbocatalysis in Liquidâ€Phase Reactions. Angewandte Chemie - International Edition, 2017, 56, 936-964.	13.8	209
16	A carbon nitride/TiO2 nanotube array heterojunction visible-light photocatalyst: synthesis, characterization, and photoelectrochemical properties. Journal of Materials Chemistry, 2012, 22, 17900.	6.7	206
17	Sulfur and nitrogen co-doped carbon nanotubes for enhancing electrochemical oxygen reduction activity in acidic and alkaline media. Journal of Materials Chemistry A, 2013, 1, 14853.	10.3	203
18	(111) TiO 2-x /Ti 3 C 2 : Synergy of active facets, interfacial charge transfer and Ti 3+ doping for enhance photocatalytic activity. Materials Research Bulletin, 2017, 89, 16-25.	5.2	190

#	Article	IF	CITATIONS
19	Preparation and characterization of Cu2O/TiO2 nano–nano heterostructure photocatalysts. Catalysis Communications, 2009, 10, 1839-1843.	3.3	170
20	Electronic synergism of pyridinic- and graphitic-nitrogen on N-doped carbons for the oxygen reduction reaction. Chemical Science, 2019, 10, 1589-1596.	7.4	170
21	MnO ₂ /CNT Supported Pt and PtRu Nanocatalysts for Direct Methanol Fuel Cells. Langmuir, 2009, 25, 7711-7717.	3.5	169
22	Adsorption characteristic of acidified carbon nanotubes for heavy metal Pb(II) in aqueous solution. Materials Science & Engineering A: Structural Materials: Properties, Microstructure and Processing, 2007, 466, 201-206.	5.6	165
23	Preparation of nitrogen-doped titanium dioxide with visible-light photocatalytic activity using a facile hydrothermal method. Journal of Physics and Chemistry of Solids, 2008, 69, 1657-1664.	4.0	163
24	Regulating Electron–Hole Separation to Promote Photocatalytic H ₂ Evolution Activity of Nanoconfined Ru/MXene/TiO ₂ Catalysts. ACS Nano, 2020, 14, 14181-14189.	14.6	160
25	Pt nanoparticles interacting with graphitic nitrogen of N-doped carbon nanotubes: Effect of electronic properties on activity for aerobic oxidation of glycerol and electro-oxidation of CO. Journal of Catalysis, 2015, 325, 136-144.	6.2	154
26	Revealing the enhanced catalytic activity of nitrogen-doped carbon nanotubes for oxidative dehydrogenation of propane. Chemical Communications, 2013, 49, 8151.	4.1	149
27	Hexavalent chromium removal over magnetic carbon nanoadsorbents: synergistic effect of fluorine and nitrogen co-doping. Journal of Materials Chemistry A, 2018, 6, 13062-13074.	10.3	145
28	Selective Allylic Oxidation of Cyclohexene Catalyzed by Nitrogen-Doped Carbon Nanotubes. ACS Catalysis, 2014, 4, 1617-1625.	11.2	143
29	Porous Mn2O3 microsphere as a superior anode material for lithium ion batteries. RSC Advances, 2012, 2, 4645.	3.6	142
30	Electrochemical Reduction of CO ₂ into Tunable Syngas Production by Regulating the Crystal Facets of Earth-Abundant Zn Catalyst. ACS Applied Materials & Interfaces, 2018, 10, 20530-20539.	8.0	141
31	Synthesis and characterization of sulfonated single-walled carbon nanotubes and their performance as solid acid catalyst. Journal of Solid State Chemistry, 2008, 181, 432-438.	2.9	138
32	Electrodeposition preparation of Ag loaded N-doped TiO2 nanotube arrays with enhanced visible light photocatalytic performance. Catalysis Communications, 2011, 12, 689-693.	3.3	138
33	Efficient electrochemical reduction of CO2 into CO promoted by sulfur vacancies. Nano Energy, 2019, 60, 43-51.	16.0	136
34	Synthesis of porous Fe3O4/g-C3N4 nanospheres as highly efficient and recyclable photocatalysts. Materials Research Bulletin, 2013, 48, 1447-1452.	5.2	132
35	Enhanced photocatalytic CO2 reduction in H2O vapor by atomically thin Bi2WO6 nanosheets with hydrophobic and nonpolar surface. Applied Catalysis B: Environmental, 2021, 283, 119630.	20.2	131
36	Kinetically Controlled Side-Wall Functionalization of Carbon Nanotubes by Nitric Acid Oxidation. Journal of Physical Chemistry C, 2008, 112, 6758-6763.	3.1	128

#	Article	IF	CITATIONS
37	Carbon nitride polymer sensitized TiO2 nanotube arrays with enhanced visible light photoelectrochemical and photocatalytic performance. Chemical Communications, 2011, 47, 10323.	4.1	128
38	Electron transfer dependent catalysis of Pt on N-doped carbon nanotubes: Effects of synthesis method on metal-support interaction. Journal of Catalysis, 2017, 348, 100-109.	6.2	126
39	One-pot melamine derived nitrogen doped magnetic carbon nanoadsorbents with enhanced chromium removal. Carbon, 2016, 109, 640-649.	10.3	125
40	Nitrogen doped carbon nanotubes with encapsulated ferric carbide as excellent electrocatalyst for oxygen reduction reaction in acid and alkaline media. Journal of Power Sources, 2015, 286, 495-503.	7.8	121
41	Electrodeposition of polyhedral Cu2O on TiO2 nanotube arrays for enhancing visible light photocatalytic performance. Electrochemistry Communications, 2011, 13, 861-864.	4.7	120
42	Novel phosphorus-doped multiwalled nanotubes with high electrocatalytic activity for O2 reduction in alkaline medium. Catalysis Communications, 2011, 16, 35-38.	3.3	114
43	Preparation of aluminum foil-supported nano-sized ZnO thin films and its photocatalytic degradation to phenol under visible light irradiation. Materials Research Bulletin, 2006, 41, 2123-2129.	5.2	113
44	Promoting role of bismuth and antimony on Pt catalysts for the selective oxidation of glycerol to dihydroxyacetone. Journal of Catalysis, 2016, 335, 95-104.	6.2	110
45	Photoelectrochemical Characterization of Hydrogenated TiO ₂ Nanotubes as Photoanodes for Sensing Applications. ACS Applied Materials & Interfaces, 2013, 5, 11129-11135.	8.0	108
46	Facile synthesis of MnO2/CNT nanocomposite and its electrochemical performance for supercapacitors. Materials Science and Engineering B: Solid-State Materials for Advanced Technology, 2011, 176, 1073-1078.	3.5	105
47	Synthesis and characterization of g-C3N4/Cu2O composite catalyst with enhanced photocatalytic activity under visible light irradiation. Materials Research Bulletin, 2014, 56, 19-24.	5.2	104
48	Sulfonated carbon nanotubes as a strong protonic acid catalyst. Carbon, 2005, 43, 2405-2408.	10.3	102
49	Elucidating Interaction between Palladium and N-Doped Carbon Nanotubes: Effect of Electronic Property on Activity for Nitrobenzene Hydrogenation. ACS Catalysis, 2019, 9, 2893-2901.	11.2	101
50	Methanol electrocatalytic oxidation on highly dispersed Pt/sulfonated-carbon nanotubes catalysts. Electrochemistry Communications, 2006, 8, 499-504.	4.7	100
51	Facile preparation of RuO2/CNT catalyst by a homogenous oxidation precipitation method and its catalytic performance. Applied Catalysis A: General, 2007, 321, 190-197.	4.3	100
52	"In situ―XPS study of band structures at Cu2O/TiO2 heterojunctions interface. Surface Science, 2009, 603, 2825-2834.	1.9	100
53	Selective etching of gold nanorods by ferric chloride at room temperature. CrystEngComm, 2009, 11, 2797.	2.6	100
54	Aerobic Liquidâ€Phase Oxidation of Ethylbenzene to Acetophenone Catalyzed by Carbon Nanotubes. ChemCatChem, 2013, 5, 1578-1586.	3.7	97

#	Article	IF	CITATIONS
55	Effect of the metal foam materials on the performance of methanol steam micro-reformer for fuel cells. Applied Catalysis A: General, 2007, 327, 106-113.	4.3	96
56	Aerobic oxidation of benzyl alcohol to benzaldehyde catalyzed by carbon nanotubes without any promoter. Chemical Engineering Journal, 2014, 240, 434-442.	12.7	96
57	Non-noble metal copper nanoparticles-decorated TiO 2 nanotube arrays with plasmon-enhanced photocatalytic hydrogen evolution under visible light. International Journal of Hydrogen Energy, 2015, 40, 303-310.	7.1	95
58	Low temperature solvothermal synthesis of anatase TiO2 single crystals with wholly {100} and {001} faceted surfaces. Journal of Materials Chemistry, 2012, 22, 23906.	6.7	91
59	Autothermal reforming of ethanol for hydrogen production over perovskite LaNiO3. Chemical Engineering Journal, 2010, 160, 333-339.	12.7	89
60	AgI/TiO2 nanobelts monolithic catalyst with enhanced visible light photocatalytic activity. Journal of Hazardous Materials, 2015, 284, 207-214.	12.4	87
61	A bi-functional Co–CaO–Ca 12 Al 14 O 33 catalyst for sorption-enhanced steam reforming of glycerol to high-purity hydrogen. Chemical Engineering Journal, 2016, 286, 329-338.	12.7	81
62	Designing efficient TiO2-based photoelectrocatalysis systems for chemical engineering and sensing. Chemical Engineering Journal, 2020, 381, 122605.	12.7	81
63	Identifying active sites of CoNC/CNT from pyrolysis of molecularly defined complexes for oxidative esterification and hydrogenation reactions. Catalysis Science and Technology, 2016, 6, 1007-1015.	4.1	80
64	Bifunctional CdS@Co ₉ S ₈ /Ni ₃ S ₂ catalyst for efficient electrocatalytic and photo-assisted electrocatalytic overall water splitting. Journal of Materials Chemistry A, 2020, 8, 3083-3096.	10.3	78
65	Selective liquid phase oxidation of benzyl alcohol catalyzed by carbon nanotubes. Chemical Engineering Journal, 2012, 204-206, 98-106.	12.7	77
66	Novel silicon-doped, silicon and nitrogen-codoped carbon nanomaterials with high activity for the oxygen reduction reaction in alkaline medium. Journal of Materials Chemistry A, 2015, 3, 3289-3293.	10.3	77
67	ZnO/CdS/PbS nanotube arrays with multi-heterojunctions for efficient visible-light-driven photoelectrochemical hydrogen evolution. Chemical Engineering Journal, 2019, 362, 658-666.	12.7	76
68	High performance hydrogenated TiO2 nanorod arrays as a photoelectrochemical sensor for organic compounds under visible light. Electrochemistry Communications, 2014, 40, 24-27.	4.7	74
69	Engineering highly active Ag/Nb2O5@Nb2CT (MXene) photocatalysts via steering charge kinetics strategy. Chemical Engineering Journal, 2021, 421, 128766.	12.7	73
70	CdS@Ni ₃ S ₂ core–shell nanorod arrays on nickel foam: a multifunctional catalyst for efficient electrochemical catalytic, photoelectrochemical and photocatalytic H ₂ production reaction. Journal of Materials Chemistry A, 2019, 7, 2560-2574.	10.3	71
71	Efficient and stable oxidative steam reforming of ethanol for hydrogen production: Effect of in situ dispersion of Ir over Ir/La2O3. Journal of Catalysis, 2010, 269, 281-290.	6.2	70
72	Novel Highly Active Anatase/Rutile TiO ₂ Photocatalyst with Hydrogenated Heterophase Interface Structures for Photoelectrochemical Water Splitting into Hydrogen. ACS Sustainable Chemistry and Engineering, 2018, 6, 10823-10832.	6.7	69

#	Article	IF	CITATIONS
73	Metal-free carbocatalysis for electrochemical oxygen reduction reaction: Activity origin and mechanism. Journal of Energy Chemistry, 2020, 48, 308-321.	12.9	69
74	Revealing active-site structure of porous nitrogen-defected carbon nitride for highly effective photocatalytic hydrogen evolution. Chemical Engineering Journal, 2019, 373, 687-699.	12.7	68
75	A new insight into regulating high energy facets of rutile TiO2. Journal of Materials Chemistry A, 2013, 1, 4182.	10.3	67
76	Low-overpotential selective reduction of CO2 to ethanol on electrodeposited Cu Au nanowire arrays. Journal of Energy Chemistry, 2019, 37, 176-182.	12.9	66
77	MnO2-decorated N-doped carbon nanotube with boosted activity for low-temperature oxidation of formaldehyde. Journal of Hazardous Materials, 2020, 396, 122750.	12.4	66
78	Pt supported on phosphorus-doped carbon nanotube as an anode catalyst for direct methanol fuel cells. Electrochemistry Communications, 2012, 16, 73-76.	4.7	65
79	The Evolution from a Typical Type-I CdS/ZnS to Type-II and Z-Scheme Hybrid Structure for Efficient and Stable Hydrogen Production under Visible Light. ACS Sustainable Chemistry and Engineering, 2020, 8, 4537-4546.	6.7	65
80	High efficient conversion of cellulose to polyols with Ru/CNTs as catalyst. Renewable Energy, 2012, 37, 192-196.	8.9	64
81	Morphology Effect of Ir/La ₂ O ₂ CO ₃ Nanorods with Selectively Exposed {110} Facets in Catalytic Steam Reforming of Glycerol. ACS Catalysis, 2015, 5, 1155-1163.	11.2	64
82	Electron-Rich Ruthenium on Nitrogen-Doped Carbons Promoting Levulinic Acid Hydrogenation to γ-Valerolactone: Effect of Metal–Support Interaction. ACS Sustainable Chemistry and Engineering, 2019, 7, 16501-16510.	6.7	64
83	Co3S4/NCNTs: A catalyst for oxygen evolution reaction. Catalysis Today, 2015, 245, 74-78.	4.4	62
84	Lignin derived multi-doped (N, S, Cl) carbon materials as excellent electrocatalyst for oxygen reduction reaction in proton exchange membrane fuel cells. Journal of Energy Chemistry, 2020, 44, 106-114.	12.9	62
85	Phosphorus-doped carbon nanotubes supported low Pt loading catalyst for the oxygen reduction reaction in acidic fuel cells. Journal of Power Sources, 2014, 268, 171-175.	7.8	61
86	A facile fabrication of hierarchical Ag nanoparticles-decorated N-TiO 2 with enhanced photocatalytic hydrogen production under solar light. International Journal of Hydrogen Energy, 2016, 41, 3446-3455.	7.1	61
87	Tailoring the geometric and electronic structure of tungsten oxide with manganese or vanadium doping toward highly efficient electrochemical and photoelectrochemical water splitting. Journal of Materials Chemistry A, 2019, 7, 6161-6172.	10.3	61
88	A novel bicomponent Co ₃ S ₄ /Co@C cocatalyst on CdS, accelerating charge separation for highly efficient photocatalytic hydrogen evolution. Green Chemistry, 2020, 22, 238-247.	9.0	61
89	Boosting photocatalytic hydrogen evolution using a noble-metal-free co-catalyst: CuNi@C with oxygen-containing functional groups. Applied Catalysis B: Environmental, 2021, 291, 120139.	20.2	61
90	Thermal stability of gold nanorods in an aqueous solution. Colloids and Surfaces A: Physicochemical and Engineering Aspects, 2010, 372, 177-181.	4.7	59

#	Article	IF	CITATIONS
91	Crystal engineering and SERS properties of Ag–Fe3O4 nanohybrids: from heterodimer to core–shell nanostructures. Journal of Materials Chemistry, 2011, 21, 17930.	6.7	59
92	From chicken feather to nitrogen and sulfur co-doped large surface bio-carbon flocs: an efficient electrocatalyst for oxygen reduction reaction. Electrochimica Acta, 2016, 213, 273-282.	5.2	59
93	Confined Iron Nanowires Enhance the Catalytic Activity of Carbon Nanotubes in the Aerobic Oxidation of Cyclohexane. ChemSusChem, 2012, 5, 1213-1217.	6.8	58
94	Co9S8-porous carbon spheres as bifunctional electrocatalysts with high activity and stability for oxygen reduction and evolution reactions. Electrochimica Acta, 2018, 265, 32-40.	5.2	58
95	Phosphorus doped Co9S8@CS as an excellent air-electrode catalyst for zinc-air batteries. Chemical Engineering Journal, 2020, 381, 122683.	12.7	58
96	Wearable self-powered human motion sensors based on highly stretchable quasi-solid state hydrogel. Nano Energy, 2021, 88, 106272.	16.0	58
97	Noble-metal-based high-entropy-alloy nanoparticles for electrocatalysis. Journal of Energy Chemistry, 2022, 68, 721-751.	12.9	58
98	The role of RuO2 in the electrocatalytic oxidation of methanol for direct methanol fuel cell. Catalysis Communications, 2009, 10, 533-537.	3.3	57
99	Visible light active pure rutile TiO2 photoanodes with 100% exposed pyramid-shaped (111) surfaces. Nano Research, 2012, 5, 762-769.	10.4	57
100	Enhancing the catalytic activity of carbon nanotubes by nitrogen doping in the selective liquid phase oxidation of benzyl alcohol. Catalysis Communications, 2013, 39, 44-49.	3.3	56
101	The effect of edge carbon of carbon nanotubes on the electrocatalytic performance of oxygen reduction reaction. Electrochemistry Communications, 2014, 40, 5-8.	4.7	55
102	Nitrogen-doped graphene-supported cobalt carbonitride@oxide core–shell nanoparticles as a non-noble metal electrocatalyst for an oxygen reduction reaction. Journal of Materials Chemistry A, 2015, 3, 1142-1151.	10.3	55
103	Synergistic Effect of Nitrogen Dopants on Carbon Nanotubes on the Catalytic Selective Epoxidation of Styrene. ACS Catalysis, 2020, 10, 129-137.	11.2	55
104	Understanding of nitrogen fixation electro catalyzed by molybdenum–iron carbide through the experiment and theory. Nano Energy, 2020, 68, 104374.	16.0	55
105	Synthesis of Cu2O nanoboxes, nanocubes and nanospheres by polyol process and their adsorption characteristic. Materials Research Bulletin, 2008, 43, 3047-3053.	5.2	54
106	Electrodeposition preparation of octahedral-Cu2O-loaded TiO2 nanotube arrays for visible light-driven photocatalysis. Scripta Materialia, 2010, 63, 159-161.	5.2	54
107	Carbon nanotubes as catalyst for the aerobic oxidation of cumene to cumene hydroperoxide. Applied Catalysis A: General, 2014, 478, 1-8.	4.3	54
108	Enhancing hydrogen evolution reaction through modulating electronic structure of self-supported NiFe LDH. Catalysis Science and Technology, 2020, 10, 4184-4190.	4.1	53

#	Article	IF	CITATIONS
109	The influence of the electrodeposition potential on the morphology of Cu2O/TiO2 nanotube arrays and their visible-light-driven photocatalytic activity for hydrogen evolution. International Journal of Hydrogen Energy, 2013, 38, 13866-13871.	7.1	52
110	Effect of Experimental Operations on the Limiting Current Density of Oxygen Reduction Reaction Evaluated by Rotatingâ€Disk Electrode. ChemElectroChem, 2020, 7, 1107-1114.	3.4	52
111	Preparation of phosphorus-doped carbon nanospheres and their electrocatalytic performance for O2 reduction. Journal of Natural Gas Chemistry, 2012, 21, 257-264.	1.8	51
112	Electrodeposition of Cu2O/g-C3N4 heterojunction film on an FTO substrate for enhancing visible light photoelectrochemical water splitting. Chinese Journal of Catalysis, 2017, 38, 365-371.	14.0	51
113	Antibacterial Activities of Novel Dithiocarbamate-Containing 4 <i>H</i> -Chromen-4-one Derivatives. Journal of Agricultural and Food Chemistry, 2020, 68, 5641-5647.	5.2	51
114	Preparation of nitrogen doped TiO2 photocatalyst by oxidation of titanium nitride with H2O2. Materials Research Bulletin, 2011, 46, 840-844.	5.2	50
115	Effect of nitrogen-doping temperature on the structure and photocatalytic activity of the B,N-doped TiO2. Journal of Solid State Chemistry, 2011, 184, 134-140.	2.9	50
116	Manipulating photocatalytic pathway and activity of ternary Cu2O/(001)TiO2@Ti3C2Tx catalysts for H2 evolution: Effect of surface coverage. International Journal of Hydrogen Energy, 2019, 44, 29975-29985.	7.1	50
117	Development of stable PtRu catalyst coated with manganese dioxide for electrocatalytic oxidation of methanol. Electrochemistry Communications, 2010, 12, 1210-1213.	4.7	49
118	Steam Reforming of Oxygenate Fuels for Hydrogen Production: A Thermodynamic Study. Energy & Fuels, 2011, 25, 2643-2650.	5.1	49
119	Preparation of B, N-codoped nanotube arrays and their enhanced visible light photoelectrochemical performances. Electrochemistry Communications, 2011, 13, 121-124.	4.7	48
120	Competitive adsorption on single-atom catalysts: Mechanistic insights into the aerobic oxidation of alcohols over Co N C. Journal of Catalysis, 2019, 377, 283-292.	6.2	48
121	Syngas production by dry reforming of the mixture of glycerol and ethanol with CaCO3. Journal of Energy Chemistry, 2020, 43, 90-97.	12.9	48
122	Antibacterial and Antiviral Activities of 1,3,4-Oxadiazole Thioether 4 <i>H</i> -Chromen-4-one Derivatives. Journal of Agricultural and Food Chemistry, 2021, 69, 11085-11094.	5.2	48
123	A simple preparation of nitrogen doped titanium dioxide nanocrystals with exposed (001) facets with high visible light activity. Chemical Communications, 2012, 48, 600-602.	4.1	46
124	sp2- and sp3-hybridized carbon materials as catalysts for aerobic oxidation of cyclohexane. Catalysis Science and Technology, 2013, 3, 2654.	4.1	46
125	Cu(OH)2-modified TiO2 nanotube arrays for efficient photocatalytic hydrogen production. International Journal of Hydrogen Energy, 2013, 38, 7241-7245.	7.1	46
126	Novel highly efficient alumina-supported cobalt nitride catalyst for preferential CO oxidation at high temperatures. International Journal of Hydrogen Energy, 2011, 36, 1955-1959.	7.1	45

#	Article	IF	CITATIONS
127	Mechanistic Insight into the Catalytic Oxidation of Cyclohexane over Carbon Nanotubes: Kinetic and In Situ Spectroscopic Evidence. Chemistry - A European Journal, 2013, 19, 9818-9824.	3.3	44
128	Superior cycle stability of graphene nanosheets prepared by freeze-drying process as anodes for lithium-ion batteries. Journal of Power Sources, 2014, 254, 198-203.	7.8	44
129	Preparation of nitrogen and sulfur co-doped ultrathin graphitic carbon via annealing bagasse lignin as potential electrocatalyst towards oxygen reduction reaction in alkaline and acid media. Journal of Energy Chemistry, 2019, 34, 33-42.	12.9	44
130	Surface oxidized nano-cobalt wrapped by nitrogen-doped carbon nanotubes for efficient purification of organic wastewater. Separation and Purification Technology, 2021, 259, 118098.	7.9	43
131	Design, Synthesis, Antibacterial Activity, Antiviral Activity, and Mechanism of Myricetin Derivatives Containing a Quinazolinone Moiety. ACS Omega, 2021, 6, 30826-30833.	3.5	43
132	Mesoporous zinc-blende ZnS nanoparticles: synthesis, characterization and superior photocatalytic properties. Nanotechnology, 2008, 19, 255603.	2.6	42
133	Highly uniform and monodisperse carbon nanospheres enriched with cobalt–nitrogen active sites as a potential oxygen reduction electrocatalyst. Journal of Power Sources, 2017, 346, 80-88.	7.8	42
134	Nickel Nanoparticles Encapsulated in Nitrogen-Doped Carbon Nanotubes as Excellent Bifunctional Oxygen Electrode for Fuel Cell and Metal–Air Battery. ACS Sustainable Chemistry and Engineering, 2018, 6, 15108-15118.	6.7	42
135	Selective oxidation of glycerol over supported noble metal catalysts. Catalysis Today, 2021, 365, 162-171.	4.4	42
136	Thermodynamic analysis of hydrogen generation via oxidative steam reforming of glycerol. Renewable Energy, 2011, 36, 2120-2127.	8.9	41
137	Catalytic wet air oxidation of phenol over carbon nanotubes: Synergistic effect of carboxyl groups and edge carbons. Carbon, 2018, 133, 464-473.	10.3	41
138	Highly efficient and acid-corrosion resistant nitrogen doped magnetic carbon nanotubes for the hexavalent chromium removal with subsequent reutilization. Chemical Engineering Journal, 2019, 361, 547-558.	12.7	41
139	CdS@Ni3S2 for efficient and stable photo-assisted electrochemical (P-EC) overall water splitting. Chemical Engineering Journal, 2021, 405, 126231.	12.7	41
140	Chemical Synthesis, Structural Characterization, Optical Properties, and Photocatalytic Activity of Ultrathin ZnSe Nanorods. Chemistry - A European Journal, 2011, 17, 8663-8670.	3.3	40
141	A kinetics study on cumene oxidation catalyzed by carbon nanotubes: Effect of N-doping. Chemical Engineering Science, 2018, 177, 391-398.	3.8	40
142	Revealing the Relationship between Photocatalytic Properties and Structure Characteristics of TiO ₂ Reduced by Hydrogen and Carbon Monoxide Treatment. ChemSusChem, 2018, 11, 2766-2775.	6.8	40
143	Platinum-based ternary catalysts for the electrooxidation of ethanol. Particuology, 2021, 58, 169-186.	3.6	39
144	Tuning the Selectivity in the Aerobic Oxidation of Cumene Catalyzed by Nitrogenâ€Doped Carbon Nanotubes, ChemCatChem, 2014, 6, 555-560.	3.7	38

#	Article	IF	CITATIONS
145	Co-Cu-CaO catalysts for high-purity hydrogen from sorption-enhanced steam reforming of glycerol. Applied Catalysis A: General, 2017, 533, 9-16.	4.3	38
146	In-situ photo-deposition CuO1â^' cluster on TiO2 for enhanced photocatalytic H2-production activity. International Journal of Hydrogen Energy, 2017, 42, 19942-19950.	7.1	38
147	Calcium cobaltate: a phase-change catalyst for stable hydrogen production from bio-glycerol. Energy and Environmental Science, 2018, 11, 660-668.	30.8	38
148	CdS branched TiO2: Rods-on-rods nanoarrays for efficient photoelectrochemical (PEC) and self-bias photocatalytic (PC) hydrogen production. Journal of Power Sources, 2019, 430, 32-42.	7.8	38
149	RuO2·xH2O Supported on Carbon Nanotubes as a Highly Active Catalyst for Methanol Oxidation. Journal of Physical Chemistry C, 2008, 112, 11875-11880.	3.1	37
150	Carbokatalyse in Flüssigphasenreaktionen. Angewandte Chemie, 2017, 129, 956-985.	2.0	37
151	FeCo alloy@N-doped graphitized carbon as an efficient cocatalyst for enhanced photocatalytic H2 evolution by inducing accelerated charge transfer. Journal of Energy Chemistry, 2021, 52, 92-101.	12.9	37
152	Phase ontrollable Growth Ni <i>_x</i> P <i>_y</i> Modified CdS@Ni ₃ S ₂ Electrodes for Efficient Electrocatalytic and Enhanced Photoassisted Electrocatalytic Overall Water Splitting. Small Methods, 2021, 5, e2100878.	8.6	37
153	One‣tep Synthesis and Characterization of Gold–Hollow PbS _{<i>x</i>} Hybrid Nanoparticles. Angewandte Chemie - International Edition, 2009, 48, 3991-3995.	13.8	36
154	Energy-efficient catalytic removal of formaldehyde enabled by precisely Joule-heated Ag/Co3O4@mesoporous-carbon monoliths. Carbon, 2020, 167, 709-717.	10.3	36
155	Synergies of the crystallinity and conductive agents on the electrochemical properties of the hollow Fe3O4 spheres. Electrochimica Acta, 2012, 76, 495-503.	5.2	35
156	Design and preparation of CdS/H-3D-TiO2/Pt-wire photocatalysis system with enhanced visible-light driven H2 evolution. International Journal of Hydrogen Energy, 2017, 42, 928-937.	7.1	35
157	Co-production of high quality hydrogen and synthesis gas via sorption-enhanced steam reforming of glycerol coupled with methane reforming of carbonates. Chemical Engineering Journal, 2019, 360, 47-53.	12.7	35
158	Photoelectrochemical Characterization of a Robust TiO ₂ /BDD Heterojunction Electrode for Sensing Application in Aqueous Solutions. Langmuir, 2010, 26, 6033-6040.	3.5	34
159	Organic-free Anatase TiO2 Paste for Efficient Plastic Dye-Sensitized Solar Cells and Low Temperature Processed Perovskite Solar Cells. ACS Applied Materials & Interfaces, 2015, 7, 19431-19438.	8.0	34
160	Ni foams decorated with carbon nanotubes as catalytic stirrers for aerobic oxidation of cumene. Chemical Engineering Journal, 2016, 306, 806-815.	12.7	34
161	Chemically drilling carbon nanotubes for electrocatalytic oxygen reduction reaction. Electrochimica Acta, 2016, 190, 49-56.	5.2	34
162	Solvent effect on the allylic oxidation of cyclohexene catalyzed by nitrogen doped carbon nanotubes. Catalysis Communications, 2017, 88, 99-103.	3.3	34

#	Article	IF	CITATIONS
163	Hydrogen production via autothermal reforming of ethanol over noble metal catalysts supported on oxides. Journal of Natural Gas Chemistry, 2009, 18, 191-198.	1.8	33
164	Capacitance dependent catalytic activity of RuO2·xH2O/CNT nanocatalysts for aerobic oxidation of benzyl alcohol. Chemical Communications, 2009, , 2408.	4.1	33
165	Theoretical calculations and controllable synthesis of MoSe2/CdS-CdSe with highly active sites for photocatalytic hydrogen evolution. Chemical Engineering Journal, 2020, 383, 123133.	12.7	33
166	Enhanced methanol oxidation activity of Pt catalyst supported on the phosphorus-doped multiwalled carbon nanotubes in alkaline medium. Catalysis Communications, 2012, 22, 34-38.	3.3	32
167	Enhancing the catalytic activity of carbon nanotubes by filled iron nanowires for selective oxidation of ethylbenzene. Catalysis Communications, 2014, 51, 77-81.	3.3	32
168	Aerobic oxidation of α-pinene catalyzed by carbon nanotubes. Catalysis Science and Technology, 2015, 5, 3935-3944.	4.1	32
169	Mn ₃ O ₄ @C Nanoparticles Supported on Porous Carbon as Bifunctional Oxygen Electrodes and their Electrocatalytic Mechanism. ChemElectroChem, 2019, 6, 359-368.	3.4	32
170	The zinc vacancy induced CdS/ZnS Z-scheme structure as a highly stable photocatalyst for hydrogen production. Journal of Alloys and Compounds, 2021, 888, 161620.	5.5	32
171	Assessment and optimization of the mass-transfer limitation in a metal foam methanol microreformer. Applied Catalysis A: General, 2008, 337, 155-162.	4.3	31
172	Design, synthesis and the electrochemical performance of MnO2/C@CNT as supercapacitor material. Materials Research Bulletin, 2013, 48, 3389-3393.	5.2	31
173	A Novel Carbonâ€Encapsulated Cobaltâ€Tungsten Carbide as Electrocatalyst for Oxygen Reduction Reaction in Alkaline Media. Fuel Cells, 2013, 13, 387-391.	2.4	30
174	Preparation of boron and phosphor co-doped TiO2 nanotube arrays and their photoelectrochemical property. Electrochemistry Communications, 2012, 19, 127-130.	4.7	29
175	Preparation of Bi2Ti2O7/TiO2 nanocomposites and their photocatalytic performance under visible light irradiation. Materials and Design, 2015, 86, 152-155.	7.0	29
176	Magnetic Fe3C@C nanoparticles as a novel cocatalyst for boosting visible-light-driven photocatalytic performance of g-C3N4. International Journal of Hydrogen Energy, 2019, 44, 26970-26981.	7.1	29
177	Formation of Lattice-Dislocated Zinc Oxide via Anodic Corrosion for Electrocatalytic CO ₂ Reduction to Syngas with a Potential-Dependent CO:H ₂ Ratio. ACS Applied Materials & Interfaces, 2020, 12, 30466-30473.	8.0	29
178	Synthesis of cationic hemicellulosic derivatives with a low degree of substitution in dimethyl sulfoxide media. Journal of Applied Polymer Science, 2008, 109, 2711-2717.	2.6	28
179	Facile Preparation of an Excellent Pt/RuO ₂ â€MnO ₂ /CNTs Nanocatalyst for Anodes of Direct Methanol Fuel Cells. Fuel Cells, 2011, 11, 301-308.	2.4	28
180	Controlled preparation of Ag–Cu2O nanocorncobs and their enhanced photocatalytic activity under visible light. Materials Research Bulletin, 2015, 70, 296-302.	5.2	28

#	Article	IF	CITATIONS
181	Computational Screening of Metal–Organic Framework Membranes for the Separation of 15 Gas Mixtures. Nanomaterials, 2019, 9, 467.	4.1	28
182	Oxygen Doping in Graphitic Carbon Nitride for Enhanced Photocatalytic Hydrogen Evolution. ChemSusChem, 2020, 13, 5041-5049.	6.8	28
183	Biomass-Derived Nitrogen-Doped Porous Carbons Activated by Magnesium Chloride as Ultrahigh-Performance Supercapacitors. Industrial & Engineering Chemistry Research, 2020, 59, 21756-21767.	3.7	28
184	Hydrogen Production from Sorption-Enhanced Steam Reforming of Phenol over a Ni–Ca–Al–O Bifunctional Catalyst. ACS Sustainable Chemistry and Engineering, 2020, 8, 7111-7120.	6.7	28
185	One-pot synthesis of Ru/Nb2O5@Nb2C ternary photocatalysts for water splitting by harnessing hydrothermal redox reactions. Applied Catalysis B: Environmental, 2022, 303, 120910.	20.2	28
186	Fabrication of uniformly dispersed Ag nanoparticles loaded TiO 2 nanotube arrays for enhancing photoelectrochemical and photocatalytic performances under visible light irradiation. Materials Research Bulletin, 2014, 60, 130-136.	5.2	27
187	Si-doped carbon nanotubes as efficient metal-free electrocatalysts for O2 reduction in alkaline medium. Materials Letters, 2015, 158, 32-35.	2.6	27
188	Enhanced activity and durability of platinum anode catalyst by the modification of cobalt phosphide for direct methanol fuel cells. Electrochimica Acta, 2015, 185, 178-183.	5.2	27
189	Branched hydrogenated TiO 2 nanorod arrays for improving photocatalytic hydrogen evolution performance under simulated solar light. International Journal of Hydrogen Energy, 2016, 41, 20192-20197.	7.1	27
190	Effect of calcium dopant on catalysis of Ir/La2O3 for hydrogen production by oxidative steam reforming of glycerol. Applied Catalysis B: Environmental, 2012, 127, 89-98.	20.2	26
191	Controllable Preparation of Holey Graphene and Electrocatalytic Performance for Oxygen Reduction Reaction. Electrochimica Acta, 2017, 228, 203-213.	5.2	26
192	Sorption-enhanced steam reforming of glycerol over Ni Cu Ca Al catalysts for producing fuel-cell grade hydrogen. International Journal of Hydrogen Energy, 2017, 42, 17446-17456.	7.1	26
193	Design of cocatalyst loading position for photocatalytic water splitting into hydrogen in electrolyte solutions. International Journal of Hydrogen Energy, 2018, 43, 5551-5560.	7.1	26
194	Preparation of CdS-CoSx photocatalysts and their photocatalytic and photoelectrochemical characteristics for hydrogen production. International Journal of Hydrogen Energy, 2019, 44, 27795-27805.	7.1	26
195	Heterostructured CoO/3D-TiO2 nanorod arrays for photoelectrochemical water splitting hydrogen production. Journal of Solid State Electrochemistry, 2017, 21, 455-461.	2.5	25
196	Preparation of carbon nanotube-supported Fe2O3 catalysts and their catalytic activities for ethylbenzene dehydrogenation. New Carbon Materials, 2007, 22, 213-217.	6.1	24
197	Boron and nitrogen-codoped TiO2 nanorods: Synthesis, characterization, and photoelectrochemical properties. Journal of Solid State Chemistry, 2011, 184, 3002-3007.	2.9	24
198	A Novel Carbothermal Synthesis Route for Carbon Nanotube Supported Fe2P Nanoparticles. Topics in Catalysis, 2012, 55, 1040-1045.	2.8	24

#	Article	IF	CITATIONS
199	Enhancing the photocatalytic efficiency of TiO 2 nanotube arrays for H 2 production by using non-noble metal cobalt as co-catalyst. Materials Letters, 2016, 165, 37-40.	2.6	24
200	New route of fabricating BiOI and Bi 2 O 3 supported TiO 2 nanotube arrays via the electrodeposition of bismuth nanoparticles for photocatalytic degradation of acid orange II. Materials Chemistry and Physics, 2017, 196, 237-244.	4.0	24
201	Dual modification of TiO 2 nanorods for selective photoelectrochemical detection of organic compounds. Sensors and Actuators B: Chemical, 2017, 250, 307-314.	7.8	24
202	Structural stability and mutual transformations of molybdenum carbide, nitride and phosphide. Materials Research Bulletin, 2011, 46, 1938-1941.	5.2	23
203	Nanocrystal Cu2O-loaded TiO2 nanotube array films as high-performance visible-light bactericidal photocatalyst. Applied Microbiology and Biotechnology, 2012, 96, 1201-1207.	3.6	23
204	Facile preparation of hierarchical TiO ₂ nanowire–nanoparticle/nanotube architecture for highly efficient dye-sensitized solar cells. Journal of Materials Chemistry A, 2015, 3, 20366-20374.	10.3	23
205	Effect of the surface roughness of copper substrate on three-dimensional tin electrode for electrochemical reduction of CO2 into HCOOH. Journal of CO2 Utilization, 2017, 21, 219-223.	6.8	23
206	Enhanced activity of Pt/CNTs anode catalyst for direct methanol fuel cells using Ni2P as co-catalyst. Applied Surface Science, 2018, 434, 534-539.	6.1	23
207	O ₂ and H ₂ O ₂ transformation steps for the oxygen reduction reaction catalyzed by graphitic nitrogen-doped carbon nanotubes in acidic electrolyte from first principles calculations. Physical Chemistry Chemical Physics, 2015, 17, 21950-21959.	2.8	22
208	Combining large-scale screening and machine learning to predict the metal-organic frameworks for organosulfurs removal from high-sour natural gas. APL Materials, 2019, 7, .	5.1	22
209	Trace amounts of Cu(OAc) ₂ boost the efficiency of cumene oxidation catalyzed by carbon nanotubes washed with HCl. Catalysis Science and Technology, 2020, 10, 2523-2530.	4.1	22
210	Influence of Si contents on the microstructure, mechanical and tribological properties of Cr–Si–N coatings. Ceramics International, 2016, 42, 5062-5067.	4.8	21
211	Trace iron impurities deactivate palladium supported on nitrogen-doped carbon nanotubes for nitrobenzene hydrogenation. Applied Catalysis A: General, 2017, 545, 54-63.	4.3	21
212	Valorization of Biomass Hydrolysis Waste: Activated Carbon from Humins as Exceptional Sorbent for Wastewater Treatment. Sustainability, 2018, 10, 1795.	3.2	21
213	Facile Synthesis of Cobalt and Nitrogen Coordinated Carbon Nanotube as a High-Performance Electrocatalyst for Oxygen Reduction Reaction in Both Acidic and Alkaline Media. ACS Sustainable Chemistry and Engineering, 2019, 7, 10951-10961.	6.7	21
214	Calcium Chloride Activation of Mung Bean: A Low ost, Green Route to Nâ€Đoped Porous Carbon for Supercapacitors. ChemistrySelect, 2019, 4, 3432-3439.	1.5	21
215	Highly exposed (001) facets Ni(OH)2 induced formation of nickle phosphide over cadmium sulfide nanorods for efficient photocatalytic hydrogen evolution. International Journal of Hydrogen Energy, 2020, 45, 9397-9407.	7.1	21
216	Intrinsic acid resistance and high removal performance from the incorporation of nickel nanoparticles into nitrogen doped tubular carbons for environmental remediation. Journal of Colloid and Interface Science, 2020, 566, 46-59.	9.4	21

#	Article	IF	CITATIONS
217	Porous Carbon Nanosheets Derived from ZIFâ€8 Treated with KCl as Highly Efficient Electrocatalysts for the Oxygen Reduction Reaction. Energy Technology, 2021, 9, 2100035.	3.8	21
218	Essential analysis of cyclic voltammetry of methanol electrooxidation using the differential electrochemical mass spectrometry. Journal of Power Sources, 2021, 509, 230397.	7.8	21
219	Natural light driven photovoltaic-electrolysis water splitting with 12.7% solar-to-hydrogen conversion efficiency using a two-electrode system grown with metal foam. Journal of Power Sources, 2022, 538, 231536.	7.8	21
220	Microemulsion Synthesis of Nanosized SiO2/TiO2 Particles and Their Photocatalytic Activity. Chinese Journal of Catalysis, 2007, 28, 251-256.	14.0	20
221	Chemical Synthesis, Structure Characterization, and Optical Properties of Hollow PbS _{<i>x</i>} –Solid Au Heterodimer Nanostructures. Chemistry - A European Journal, 2010, 16, 5920-5926.	3.3	20
222	Facile Formation of Branched Titanate Nanotubes to Grow a Three-Dimensional Nanotubular Network Directly on a Solid Substrate. Langmuir, 2010, 26, 1574-1578.	3.5	20
223	Controlled synthesis of octahedral Cu2O on TiO2 nanotube arrays by electrochemical deposition. Materials Chemistry and Physics, 2011, 130, 316-322.	4.0	20
224	Efficient functionalization of multi-walled carbon nanotubes by nitrogen dioxide. Materials Research Bulletin, 2013, 48, 3218-3222.	5.2	20
225	An opposite change rule in carbon nanotubes supported platinum catalyst for methanol oxidation and oxygen reduction reactions. Journal of Power Sources, 2014, 260, 1-5.	7.8	20
226	Facile and scalable synthesis of coal tar-derived, nitrogen and sulfur-codoped carbon nanotubes with superior activity for O ₂ reduction by employing an evocating agent. Journal of Materials Chemistry A, 2015, 3, 22723-22729.	10.3	20
227	Visible light photoelectrochemical properties of a hydrogenated TiO ₂ nanorod film and its application in the detection of chemical oxygen demand. RSC Advances, 2015, 5, 76315-76320.	3.6	20
228	MoS2 supported on hydrogenated TiO2 heterostructure film as photocathode for photoelectrochemical hydrogen production. International Journal of Hydrogen Energy, 2019, 44, 31008-31019.	7.1	20
229	A Nonâ€Noble Monometallic Catalyst Derived from Cu–MOFs for Highly Selective Hydrogenation of 5â€Hydroxymethylfurfural to 2,5â€Dimethylfuran. ChemistrySelect, 2019, 4, 13517-13524.	1.5	20
230	Chlorineâ€Promoted Nitrogen and Sulfur Coâ€Doped Biocarbon Catalyst for Electrochemical Carbon Dioxide Reduction. ChemElectroChem, 2020, 7, 320-327.	3.4	20
231	Mechanistic Insights into the Electrochemical Reduction of CO ₂ on Cyclo[18]carbon using Density Functional Theory Calculations. ChemElectroChem, 2020, 7, 1838-1842.	3.4	20
232	New Understanding of Selective Aerobic Oxidation of Ethylbenzene Catalyzed by Nitrogenâ€doped Carbon Nanotubes. ChemCatChem, 2021, 13, 646-655.	3.7	20
233	Photocatalysis over MXene-based hybrids: Synthesis, surface chemistry, and interfacial charge kinetics. APL Materials, 2021, 9, .	5.1	20
234	Understanding the Catalytic Sites in Porous Hexagonal Boron Nitride for the Epoxidation of Styrene. ACS Catalysis, 2021, 11, 8872-8880.	11.2	20

#	Article	IF	CITATIONS
235	Design of two kinds of branched TiO2 nano array photoanodes and their comparison of photoelectrochemical performances. Electrochimica Acta, 2017, 252, 368-373.	5.2	19
236	Deactivation and regeneration of <i>in situ</i> formed bismuth-promoted platinum catalyst for the selective oxidation of glycerol to dihydroxyacetone. New Journal of Chemistry, 2018, 42, 18837-18843.	2.8	19
237	Direct vapor-phase carbonylation of methanol at atmospheric pressure on activated carbon-supported NiCl2–CuCl2 catalysts. Catalysis Today, 2004, 93-95, 451-455.	4.4	18
238	Two-dimensional oxalate-bridged heterometallic coordination polymer: Crystal structure and thermal behavior of [NaCr(pyim)(ox)2(H2O)]·2H2O (pyim=2-(2′-pyridyl)imidazole). Inorganic Chemistry Communication, 2006, 9, 486-488.	3.9	18
239	Preparation of Ag-sensitized ZnO and its photocatalytic performance under simulated solar light. Korean Journal of Chemical Engineering, 2007, 24, 1022-1026.	2.7	18
240	The influence of ultrasound on the formation of TiO2 nanotube arrays. Materials Research Bulletin, 2010, 45, 200-204.	5.2	18
241	Hydrogen permeability of Pd–Ag membrane modules with porous stainless steel substrates. International Journal of Hydrogen Energy, 2011, 36, 1014-1026.	7.1	18
242	Pt/IrO2/CNT anode catalyst with high performance for direct methanol fuel cells. Catalysis Communications, 2013, 33, 34-37.	3.3	18
243	Novel 3-D nanoporous graphitic-C3N4 nanosheets with heterostructured modification for efficient visible-light photocatalytic hydrogen production. RSC Advances, 2014, 4, 52332-52337.	3.6	18
244	Solution growth of peony-like copper hydroxyl-phosphate (Cu 2 (OH)PO 4) flowers on Cu foil and their photocatalytic activity under visible light. Materials and Design, 2016, 100, 30-36.	7.0	18
245	Iron based dual-metal oxides on graphene for lithium-ion batteries anode: Effects of composition and morphology. Journal of Alloys and Compounds, 2016, 684, 47-54.	5.5	18
246	Unravelling the radical transition during the carbon-catalyzed oxidation of cyclohexane by in situ electron paramagnetic resonance in the liquid phase. Catalysis Science and Technology, 2017, 7, 4431-4436.	4.1	18
247	Cobalt and cobalt oxide supported on nitrogen-doped porous carbon as electrode materials for hydrogen evolution reaction. International Journal of Hydrogen Energy, 2019, 44, 3649-3657.	7.1	18
248	Unraveling the intrinsic enhancement of fluorine doping in the dual-doped magnetic carbon adsorbent for the environmental remediation. Journal of Colloid and Interface Science, 2019, 538, 327-339.	9.4	18
249	Design, synthesis, and antibacterial activity of novel myricetin derivatives containing sulfonate. Monatshefte FÃ1⁄4r Chemie, 2021, 152, 345-356.	1.8	18
250	Efficient purification of tetracycline wastewater by activated persulfate with heterogeneous Co-V bimetallic oxides. Journal of Colloid and Interface Science, 2022, 619, 188-197.	9.4	18
251	Anion-tuned self-assembly of zinc(II)–fluconazole complexes: Crystal structures, luminescent and thermal properties. Journal of Molecular Structure, 2007, 829, 161-167.	3.6	17
252	Preparation of NaxBayBiO3•nH2O and their photooxidation characteristic under visible-light irradiation. Materials Chemistry and Physics, 2009, 116, 294-299.	4.0	17

#	Article	IF	CITATIONS
253	A novel carbothermal reduction nitridation route to MoN nanoparticles on CNTs support. Journal of Materials Chemistry, 2011, 21, 6898.	6.7	17
254	Design of Pt catalyst with high electrocatalytic activity and well tolerance to methanol for oxygen reduction in acidic medium. Catalysis Communications, 2012, 29, 11-14.	3.3	17
255	Green synthesis of iron and nitrogen coâ€doped porous carbon via pyrolysing lotus root as a <scp>highâ€performance</scp> electrocatalyst for oxygen reduction reaction. International Journal of Energy Research, 2021, 45, 10393-10408.	4.5	17
256	CoMn2O4 supported on carbon nanotubes for effective low-temperature HCHO removal. Journal of Alloys and Compounds, 2021, 859, 157808.	5.5	17
257	Hydrogenated CdS nanorods arrays/FTO film: A highly stable photocatalyst for photocatalytic H2 production. International Journal of Hydrogen Energy, 2018, 43, 17696-17707.	7.1	16
258	Triple deletion of <i>clpC</i> , <i>porB</i> , and <i>mepA</i> enhances production of small ubiquitin-like modifier-N-terminal pro-brain natriuretic peptide in <i>Corynebacterium glutamicum</i> . Journal of Industrial Microbiology and Biotechnology, 2019, 46, 67-79.	3.0	16
259	Selective Catalytic Oxidation of Benzyl Alcohol to Benzaldehyde by Nitrates. Frontiers in Chemistry, 2020, 8, 151.	3.6	16
260	Defectâ€Enriched ZnO/ZnS Heterostructures Derived from Hydrozincite Intermediates for Hydrogen Evolution under Visible Light. ChemSusChem, 2022, 15, .	6.8	16
261	Auto-thermal ethanol micro-reformer with a structural Ir/La2O3/ZrO2 catalyst for hydrogen production. Chemical Engineering Journal, 2011, 167, 322-327.	12.7	15
262	Low Pt content catalyst supported on nitrogen and phosphorus-codoped carbon nanotubes for electrocatalytic O2 reaction in acidic medium. Materials Letters, 2015, 142, 115-118.	2.6	15
263	The effect of surface oxygenated groups of carbon nanotubes on liquid phase catalytic oxidation of cumene. Catalysis Science and Technology, 2016, 6, 2396-2402.	4.1	15
264	Dual Functional CuO _{1–<i>x</i>} Clusters for Enhanced Photocatalytic Activity and Stability of a Pt Cocatalyst in an Overall Water-Splitting Reaction. ACS Sustainable Chemistry and Engineering, 2018, 6, 17340-17351.	6.7	15
265	A Review of Carbon-based Non-noble Catalysts for Oxygen Reduction Reaction. Acta Chimica Sinica, 2017, 75, 943.	1.4	15
266	PtRu Catalysts on Nitrogen-Doped Carbon Nanotubes with Conformal Hydrogenated TiO ₂ Shells for Methanol Oxidation. ACS Applied Nano Materials, 2022, 5, 3275-3288.	5.0	15
267	Facile synthesis of porous hollow iron oxide nanoparticles supported on carbon nanotubes. Materials Letters, 2012, 67, 245-247.	2.6	14
268	Enhanced Activity and Durability of Nanosized Pt–SnO ₂ /IrO ₂ /CNTs Catalyst for Methanol Electrooxidation. Journal of Nanoscience and Nanotechnology, 2015, 15, 3662-3669.	0.9	14
269	Bi-functional particles for integrated thermo-chemical processes: Catalysis and beyond. Particuology, 2021, 56, 10-32.	3.6	14
270	Effects of RuO2 Content in Pt/RuO2/CNTs Nanocatalyst on the Electrocatalytic Oxidation Performance of Methanol. Chinese Journal of Catalysis, 2008, 29, 1093-1098.	14.0	13

#	Article	IF	CITATIONS
271	Deactivation and regeneration of RuO2·xH2O/CNT catalyst for aerobic oxidation of benzyl alcohol. Catalysis Communications, 2009, 10, 1752-1756.	3.3	13
272	Metal-Foam-Supported Pd/Al2O3 Catalysts for Catalytic Combustion of Methane: Effect of Interaction between Support and Catalyst. International Journal of Chemical Reactor Engineering, 2015, 13, 83-93.	1.1	13
273	Preparation and the Electrochemical Performance of MnO ₂ /PANI@CNT Composite for Supercapacitors. Journal of Nanoscience and Nanotechnology, 2015, 15, 709-714.	0.9	13
274	Superoxide Decay Pathways in Oxygen Reduction Reaction on Carbonâ€Based Catalysts Evidenced by Theoretical Calculations. ChemSusChem, 2019, 12, 1133-1138.	6.8	13
275	Reaction/separation coupled equilibrium modeling of steam methane reforming in fluidized bed membrane reactors. International Journal of Hydrogen Energy, 2010, 35, 11798-11809.	7.1	12
276	Controllable synthesis and catalytic performance of graphene-supported metal oxide nanoparticles. Chinese Journal of Catalysis, 2014, 35, 952-959.	14.0	12
277	A novel approach to the synthesis of bulk and supported β-Mo ₂ C using dimethyl ether as a carbon source. New Journal of Chemistry, 2015, 39, 4901-4908.	2.8	12
278	Co–N–C-Supported Platinum Catalyst: Synergistic Effect on the Aerobic Oxidation of Glycerol. ACS Sustainable Chemistry and Engineering, 2020, 8, 19062-19071.	6.7	12
279	Antimicrobial evaluation of myricetin derivatives containing benzimidazole skeleton against plant pathogens. Fìtoterapìâ, 2021, 149, 104804.	2.2	12
280	Catalytic Transfer Hydrogenation of Biomass-Derived 5-Hydroxymethylfurfural into 2,5-Dihydroxymethylfuran over Co/UiO-66-NH2. Catalysis Letters, 2022, 152, 361-371.	2.6	12
281	A facile one-step preparation of hierarchically-structured TiO2 nanotube array photoanodes with enhanced photocatalytic activity. Electrochemistry Communications, 2011, 13, 1151-1154.	4.7	11
282	Low-Pollution and Controllable Selective-Area Deposition of a CdS Buffering Layer on CIGS Solar Cells by a Photochemical Technique. ACS Sustainable Chemistry and Engineering, 2017, 5, 7325-7333.	6.7	11
283	Surface-structure sensitive chemical diffusivity and reactivity of CO adsorbates on noble metal electrocatalysts. Applied Catalysis B: Environmental, 2021, 281, 119522.	20.2	11
284	High-purity hydrogen production by sorption-enhanced steam reforming of iso-octane over a Pd-promoted Ni-Ca-Al-O bi-functional catalyst. Fuel, 2021, 293, 120430.	6.4	11
285	Inhibitory effect of Zn ²⁺ on the chainâ€initiation process of cumene oxidation. International Journal of Quantum Chemistry, 2021, 121, e26780.	2.0	11
286	MnO2 nanoparticles supported on CNTs for cumene oxidation: Synergistic effect and kinetic modelling. Chemical Engineering Journal, 2022, 444, 136666.	12.7	11
287	Pt/MoO3-WO3/CNTs catalyst with excellent performance for methanol electrooxidation. Chinese Journal of Catalysis, 2014, 35, 1687-1694.	14.0	10
288	Facile fabrication of highly porous photoanode at low temperature for all-plastic dye-sensitized solar cells with quasi-solid state electrolyte. Journal of Power Sources, 2014, 271, 8-15.	7.8	10

#	Article	IF	CITATIONS
289	Facile synthesis of self-assembled mesoporous CuO nanospheres and hollow Cu ₂ O microspheres with excellent adsorption performance. RSC Advances, 2014, 4, 43024-43028.	3.6	10
290	Enhanced Catalytic Activity of Carbon Nanotubes for the Oxidation of Cyclohexane by Filling with Fe, Ni, and FeNi alloy Nanowires. Australian Journal of Chemistry, 2016, 69, 689.	0.9	10
291	A robust approach to fabricate CZTSSe absorber layer for solar cells via a self-selenizations process conducted by concentrated selenium solution. Materials Research Express, 2018, 5, 016413.	1.6	10
292	Synthesis and antibacterial activity of novel myricetin derivatives containing sulfonylpiperazine. Chemical Papers, 2021, 75, 1021-1027.	2.2	10
293	Synthesis and Characterization of Novel N-doped TiO2 Photocatalyst with Visible Light Active. Chinese Journal of Chemical Physics, 2010, 23, 437-441.	1.3	9
294	Structure, characterization, and dynamic performance of a wet air oxidation catalyst Cu–Fe–La/γ-Al2O3. Chinese Journal of Chemical Engineering, 2016, 24, 1171-1177.	3.5	9
295	Production of high-purity hydrogen from paper recycling black liquor via sorption enhanced steam reforming. Green Energy and Environment, 2021, 6, 771-779.	8.7	9
296	Mechanistic Insights into the Electrochemical Reduction of CO ₂ and N ₂ on the Regulation of a Boron Nitride Defect-Derived Two-Dimensional Catalyst using Density Functional Theory Calculations. Journal of Physical Chemistry Letters, 2021, 12, 7151-7158.	4.6	9
297	Self-nitrogen-doped porous carbon prepared via pyrolysis of grass-blade without additive for oxygen reduction reaction. Diamond and Related Materials, 2022, 121, 108742.	3.9	9
298	Ni Foam Supported TiO ₂ Nanorod Arrays with CdS Branches: Type II and Zâ€ s cheme Mechanisms Coexisted Monolithic Catalyst Film for Improved Photocatalytic H ₂ Production. Solar Rrl, 2022, 6, .	5.8	9
299	Growth of Aligned Carbon Nanotubes on Large Scale by Methane Decomposition with Deactivation Inhibitor. Journal of Natural Gas Chemistry, 2007, 16, 382-388.	1.8	8
300	Preparation and Quantitative Characterization of Nitrogen-Functionalized Multiwalled Carbon Nanotubes. Chinese Journal of Catalysis, 2010, 31, 948-954.	14.0	8
301	Controllable preparation of hollow fibrous \$\$hbox {SrCO}_{{3}}\$ SrCO 3. Bulletin of Materials Science, 2019, 42, 1.	1.7	7
302	Confined Cobalt on Carbon Nanotubes in Solventâ€free Aerobic Oxidation of Ethylbenzene: Enhanced Interfacial Charge Transfer. ChemCatChem, 2022, 14, .	3.7	7
303	Heat-regulating effects of inert salts on magnesiothermic reduction preparation of silicon nanopowder for lithium storage. Ionics, 2020, 26, 1249-1259.	2.4	6
304	Solvent-Free Production of Îμ-Caprolactone from Oxidation of Cyclohexanone Catalyzed by Nitrogen-Doped Carbon Nanotubes. Industrial & Engineering Chemistry Research, 2022, 61, 2037-2044.	3.7	6
305	Effect of Inlet Flow Distributor for Reagent Equalization on Autothermal Reforming of Ethanol in a Microreformer. Industrial & Engineering Chemistry Research, 2012, 51, 10132-10139.	3.7	5
306	High-Order Interference Effect Introduced by Polarization Mode Coupling in Polarization—Maintaining Fiber and Its Identification. Sensors, 2016, 16, 419.	3.8	5

#	Article	IF	CITATIONS
307	Photoelectrochemical detection of ultra-trace fluorine ion using TiO ₂ nanorod arrays as a probe. RSC Advances, 2019, 9, 26712-26717.	3.6	5
308	Production Process Development of Pseudorabies Virus Vaccine by Using a Novel Scale-Down Model of a Fixed-Bed Bioreactor. Journal of Pharmaceutical Sciences, 2020, 109, 959-965.	3.3	5
309	Identification, repair and characterization of a benzyl alcohol-inducible promoter for recombinant proteins overexpression in Corynebacterium glutamicum. Enzyme and Microbial Technology, 2020, 141, 109651.	3.2	5
310	Effects of colloidal silica on the properties of POSS-containing fluorinated poly(styrene–acrylate)/SiO2 composite materials. Journal of Coatings Technology Research, 2021, 18, 107-116.	2.5	5
311	Non Noble-Metal Copper–Cobalt Bimetallic Catalyst for Efficient Catalysis of the Hydrogenolysis of 5-Hydroxymethylfurfural to 2,5-Dimethylfuran under Mild Conditions. ACS Omega, 2021, 6, 10910-10920.	3.5	5
312	Quantum Dot-Encoded Beads for Ultrasensitive Detection. Recent Patents on Nanotechnology, 2009, 3, 192-202.	1.3	4
313	Mechanistic Insights into Cyclic Voltammograms on Pt(111): Kinetics Simulations. ChemPhysChem, 2019, 20, 2791-2798.	2.1	4
314	Enhancing Catalytic Activity and Selectivity by Plasmon-Induced Hot Carriers. IScience, 2020, 23, 101107.	4.1	4
315	Catalytic Synthesis of Lactones from Alkanes in the Presence of Aldehydes and Carbon Nanotubes. ACS Sustainable Chemistry and Engineering, 2022, 10, 6713-6723.	6.7	4
316	High Oxygenâ€Reductionâ€Activity and Methanolâ€Tolerance Cathode Catalyst Cu/PtFe/CNTs for Direct Methanol Fuel Cells. Fuel Cells, 2010, 10, 99-105.	2.4	3
317	Synthesis and Catalytic Properties of Carbon-Nanotube-Supported RuO2 Catalyst Encapsulated in Silica Coating. Catalysis Letters, 2012, 142, 100-107.	2.6	3
318	Highly Enhanced Methanol Electrooxidation on Pt/Nâ^'CNTâ€Decorated FeP**. ChemElectroChem, 2021, 8, 2442-2448.	3.4	3
319	Design, Synthesis and Antibacterial Activity of Novel Pyrimidine ontaining 4 <i>H</i> â€Chromenâ€4â€One Derivatives**. Chemistry and Biodiversity, 2021, 18, e2100186.	2.1	3
320	First complete mitochondrial genome from the genus <i>Coptodryas</i> (Coleoptera: Curculionidae:) Tj ETQq0 () 0 _{.1} gBT /	Overlock 10 T
321	MWNTs Modified Glassy Carbon Biosensor for Glucose. , 2006, , .		2
322	Nanosized TiO ₂ synthesis by EbCDAB microemulsion. Journal of Chemical Technology and Biotechnology, 2010, 85, 860-865.	3.2	2
323	Performance of Fast Thermally Reduced Graphene Oxide for Supercapacitor. Advanced Materials Research, 0, 785-786, 783-786.	0.3	2
324	Facile Fabrication of Cobalt Oxide Nanoflowers on Ni Foam with Excellent Electrochemical Capacitive Performance. Journal of Nanoscience and Nanotechnology, 2015, 15, 9754-9759.	0.9	2

. enotherior journal of Hanoscience and Hanoteenhology, 2

#	Article	IF	CITATIONS
325	Pseudorabies virus production using a serum-free medium in fixed-bed bioreactors with low cell inoculum density. Biotechnology Letters, 2020, 42, 2551-2560.	2.2	2
326	<scp>Pt–calcium</scp> cobaltate enables sorptionâ€enhanced steam reforming of glycerol coupled with chemicalâ€looping <scp>CH₄</scp> combustion. AICHE Journal, 2021, 67, e17383.	3.6	2
327	Radical Propagation Facilitating Aerobic Oxidation of Substituted Aromatics Promoted by Tertâ€Butyl Hydroperoxide. ChemistrySelect, 2021, 6, 6895-6903.	1.5	2
328	Ce <i>_x</i> Ni _{0.5} La _{0.5-<i>x</i>} O Catalysts for Hydrogen Production by Oxidative Steam Reforming of Glycerol: Influence of the Ce-to-La Ratio. Wuli Huaxue Xuebao/ Acta Physico - Chimica Sinica, 2016, 32, 1527-1533.	4.9	2
329	Controllable Surfactantâ€free Synthesis of Colloidal Platinum Nanocuboids Enabled by Bromide Ions and Carbon Monoxide. ChemElectroChem, 2022, 9, .	3.4	2
330	Wheatâ€Flourâ€Derived Magnetic Porous Carbons by CaCl ₂ â€Activation and their Application in Cr(VI) Removal. ChemistrySelect, 2021, 6, 13215-13223.	1.5	2
331	Which Is Better for Hydrogen Evolution on Metal@MoS ₂ Heterostructures from a Theoretical Perspective: Single Atom or Monolayer?. ACS Applied Materials & Interfaces, 2022, 14, 25592-25600.	8.0	2
332	Non-Metal Doped Pd/CNTs Catalysts for Oxygen Reduction Reaction in Alkaline Medium. Advanced Materials Research, 0, 550-553, 238-242.	0.3	1
333	Facile Synthesis and Performance of Reduced Graphene Oxide/Cobalt Oxide Composite for Supercapacitor. Advanced Materials Research, 0, 785-786, 779-782.	0.3	1
334	The PhoPR two-component system responds to oxygen deficiency and regulates the pathways for energy supply in Corynebacterium glutamicum. World Journal of Microbiology and Biotechnology, 2021, 37, 160.	3.6	1
335	Unprecedented Selective Aerobic Oxidation of Alcohols to Carbonyl Compounds Over Drilled Carbon Nanotubes Assisted with Fe(NO ₃) ₃ . ACS Sustainable Chemistry and Engineering, 2022, 10, 7564-7575.	6.7	1
336	Configuration Sensitivity of Electrocatalytic Oxygen Reduction Reaction on Nitrogen-Doped Graphene. Journal of Physical Chemistry Letters, 2022, 13, 6187-6193.	4.6	1
337	Extended SOT Wavelet Packet Coding Algorithm for Remote Sensing Images. , 2007, , .		0
338	Preparation of Cu ₂ FeSnS ₄ Single Crystals by Molten Salt Method. Nanoscience and Nanotechnology Letters, 2015, 7, 398-401.	0.4	0